PRIMARY Li/SOCl$_2$ CELLS.
X. OPTIMIZATION OF D CELLS WITH RESPECT TO ENERGY DENSITY, STORABILITY AND SAFETY

A. N. DEY

P.R. Mallory and Co. Inc., Laboratory for Physical Science, Northwest Industrial Park, Burlington, Mass. 01803 (U.S.A.)

Summary

Hermetically-constructed Li/SOCl$_2$ D cells were used for the studies reported in this publication. Optimization with respect to energy density resulted in a capacity recovery of 18 - 19 A h at 3.5 volt at 25 °C, at 0.01 A corresponding to 20 W h/in.^{3} (1.24 W h/cm^3) and 300 W h/lb. (661 W h/kg). The optimization with respect to storability resulted in cells having no voltage-delays after three months of storage at 72 °C and test at −30 °C at 3.0 A. The optimization with respect to safety resulted in cells which are resistant to abuses such as shorting and force-discharge. Approaches have also been developed to stabilize the partially-discharged cells and thus prevent spontaneous explosions on storage.

Introduction

The Li/SOCl$_2$ inorganic electrolyte system [1 - 3] is capable of providing the highest energy density among all the practical electrochemical systems known to date. For this reason, we carried out a detailed investigation in order to optimize the system with respect to the important use parameters such as energy density, storability, and safety. We pursued an experimental approach instead of a numerical one involving the computation of volumes occupied by the various cell components [4]. The results of the investigation are discussed in this paper.

Energy density

We first proposed [3] the following cell reaction stoichiometry.

$$4Li + 2SOCl_2 \longrightarrow 4LiCl + SO_2 + S. \tag{1}$$
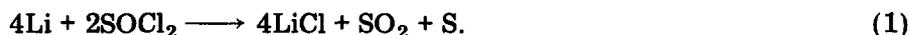
The validity of this overall stoichiometry has been confirmed by others [5, 6]. We proposed later [7, 8] that the cathodic reaction involved the forma-

tion of SO, as an unstable bi-radical which dimerizes and then decomposes to form S and SO_2

$$SOCl_2 + 2e \longrightarrow SO + 2Cl^- \tag{2}$$

$$2SO \longrightarrow (SO)_2 \tag{3}$$

$$(SO)_2 \longrightarrow S + SO_2 \tag{4}$$

giving rise to the overall stoichiometry shown in reaction (1).

Reaction (3) is most likely the rate determining reaction since it predicts the pressure buildup (due to SO_2) to be proportional to the square of the concentration of SO, which is produced electrochemically by reaction (2). Experimentally, the pressure buildup was found to be rather slow at the beginning of the discharge and rapid towards the end of the discharge according to the predicted second order kinetics as above. The final cell pressure after sufficient equilibration was always found to be that corresponding to the pressure of SO_2 generated according to cell reaction [1].

Thus, the discharge leads to the anodic dissolution of Li and the cathodic deposition of insoluble LiCl in the porous carbon cathode. The passivation of the cathode was found to be the capacity limiting feature. We determined the reaction profile [9] shown in Fig. 1 in the carbon cathode by sectioning the cathode and determining the LiCl content, and found that the diffusive choking of the cathodes by the precipitation of LiCl is the cause of the terminal polarization of the cathodes. The reaction profiles also showed that the interior and rear section of the cathode remained under-utilized during most conditions of discharge.

We carried out the energy density optimization of hermetically constructed D cells with respect to the cell construction variables: carbon cathode composition, type of carbon in the cathode, electrolyte salt concentration and electrode geometries. We found that carbon cathode compositions with 10% Teflon binder were superior to the compositions containing higher Teflon content. Since the function of the binder is to provide mechanical integrity of the cathode which expands during the discharge, as shown in Fig. 2, the least amount of Teflon needed for adequate mechanical integrity should be used. We used the above composition for all the subsequent studies.

We evaluated a series of twelve different types of carbon having diverse properties (as shown in Table 1) in terms of particle size, density, and electrical conductivity, using the Li/SOCl$_2$ D cells of hermetic construction. The efficacy of the various carbon types was evaluated by comparing the energy density outputs of the D cells at various rates, the D cells having a wound electrode structure. The width of the cathodes was kept constant at 4.45 cm (1.75 in.) for all cells. The lengths of the cathodes used were 38.1 cm (15 in.) and 50.8 cm (20 in.) for the thick and the thin cathodes, respectively. The Li anodes were sufficiently long to cover both sides of the cathodes and were stoichiometrically in excess of the SOCl$_2$ available in the cells. The energy density *vs.* discharge current plots of the D cells made with the various types
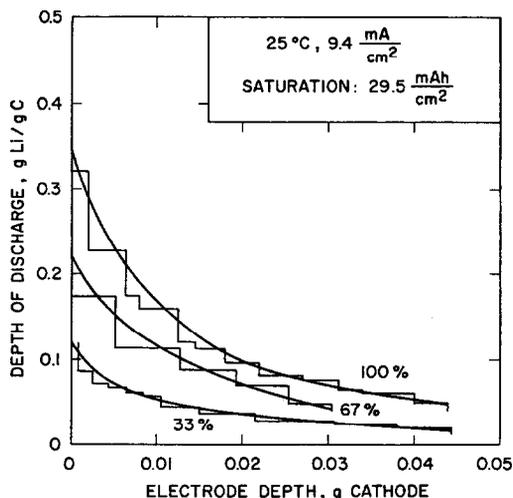
Fig. 1. Reaction profiles of carbon cathode discharged at 9.4 mA/cm^2 at 25 °C to three different depths; 100% corresponds to a capacity density of 29.5 mA h/cm^2.
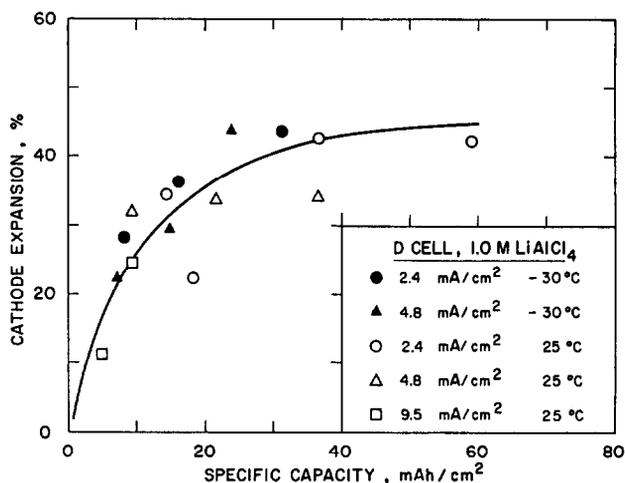
Fig. 2. Cathode expansion on discharge.

of carbons are shown in Fig. 3. The data points are shown in letters G to T representing various types of carbons. The two solid lines represent the data points of D cells with Shawinigan Black; the line with shaded circles pertains to the cells with 15 in. long electrodes and the line with unshaded circles pertains to the cells with 20 in. electrodes. It is clear that almost all types of carbon with the exception of Mogul L (J), Raven 3500 (L), and Graphite KS 10 (T) are as good as Shawinigan Black carbon (which has been used exclusively for the Li/SOCl$_2$ cells) insofar as the performance of the Li/SOCl$_2$ cells is concerned. The five types of carbon which were found to be most

TABLE 1

Types of carbons and their properties

Carbon type	Supplier	Letter desig- nation	Particle size (mμ)	BET surface area (m²/g)	Apparent density (lb./ft³)	pH	Fixed carbon (%)	Volatile matter (%)	Specific Resistance (Ohm cm)
Shawinigan Black	(Shawinigan)		43	60	1.2	–	99.5	–	0.022,0.026
Neo Spectra AG	(Columbian)	G	13	900	8	3	86.0	14.0	0.276,0.383
Elftex-12	(Cabot)	H	37	45	11	8.5	99.0	1.0	0.030,0.033
Mogul-L	(Cabot)	J	24	138	15	3.4	95.0	5.0	0.075,0.074
Raven-420	(Columbian)	K	28	70	17	9	99.6	0.4	0.044,0.037
Raven-3500	(Columbian)	L	16	319	17	3	96.2	3.8	0.095,0.111
Regal 660-R	(Cabot)	M	24	112	15	7.5	99.0	1.0	0.101,0.042
Royal Spectra	(Columbian)	N	10	1125	6	4	83.5	16.5	1.10, 1.15
Conductex-950	(Columbian)	O	21	245	10	6.5	99.2	0.8	0.044,0.051
Vulcan XC-72R	(Cabot)	P	30	254	6	7	98.0	2.0	0.021,0.035
Monarch-700	(Cabot)	R	18	200	9	8	99.0	1.0	0.167,0.054
Sterling R	(Cabot)	S	75	25	16	8.5	99.0	1.0	0.035,0.034
Graphite KS10	(Lonza)	T	10^4	~ 20	140	7.6	99.9	0.1	~ 0.002
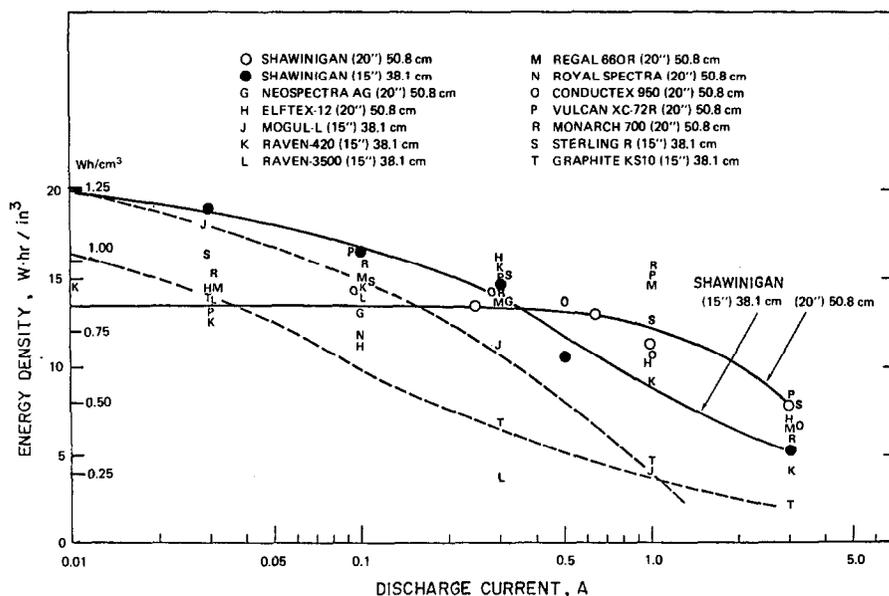
Fig. 3. Energy density of hermetic Li/SOCl$_2$ D cells made from various types of carbons at various currents at room temperature.

promising, particularly for high rate cells are Elflex-12 (H), Regal 660R (N), Vulcan XC-72R (P), Monarch 700 (R) and Sterling R (S). In addition Conductex 950 (O) also performed very well.

The virtue of using practical cells, such as a D cell, in evaluating the efficacy of various carbons as opposed to using an experimental cell having an excess electrolyte is that the performance of the cells reflects *all* the properties of the carbon that affect the cell performance. In an experimental half cell the performance of the carbon has to be expressed in terms of capacity/wt. of carbon as a function of current density and such values cannot be translated to actual cell performance. A plot of the latter type is shown in Fig. 4; the various letters represent the various data points belonging to the various types of carbons. The solid lines represent the data points belonging to Shawinigan Black for cells with both 38.1 cm (15 in.) and 50.8 cm (20 in.) long electrodes. Based on this type of analysis, one reaches the erroneous conclusion that almost all types of carbon are inferior to Shawinigan Black since all data points fall below Shawinigan Black. The reason for this is that Shawinigan Black has the lowest bulk density of all the carbons, thus having the highest capacity/carbon weight value. We have shown already that this has little bearing on the volumetric energy density of the D cell. The increase in carbon weight (with the denser carbons) results in only 1% or less increase in the cell weight. Thus the dense carbons do not significantly reduce the gravimetric energy densities. It may be noted that the preparation of the cathode mix and the cathode is an art which is more highly developed for Shawinigan Black than for the other promising carbon types, and the performances of the latter may possibly be improved significantly.
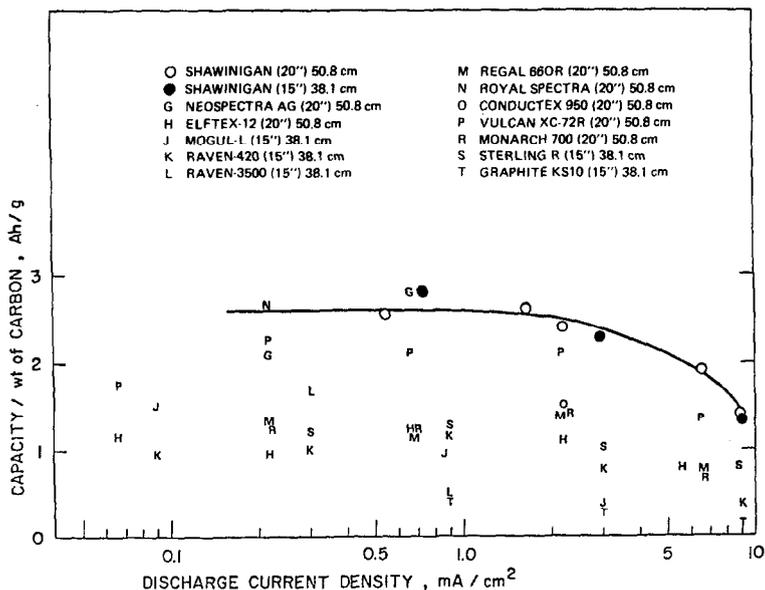
Fig. 4. Normalized plots of capacity per unit weight of carbon as a function of current density for the various types of carbons.
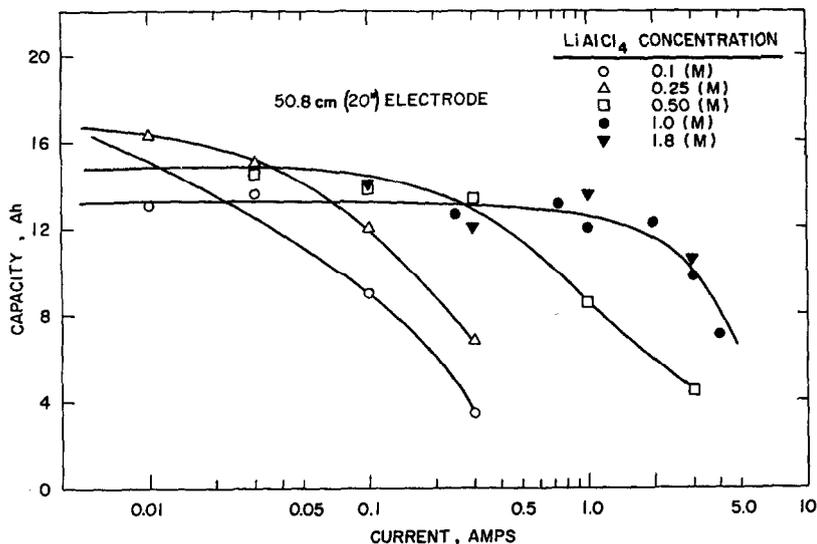
Fig. 5. Effect of salt concentration on the performance characteristics of medium rate D cells at room temperature.

We found that the concentration of the electrolyte salt (LiAlCl₄) has an important effect on the intrinsic energy density of a D cell, as shown in Fig. 5. We believe this to be due to the precipitation of the electrolyte salt towards the end of the discharge when the volume of the SOCl₂ solvent is re-

duced significantly. The precipitation results in catastrophic cathode passivation. Therefore, lower salt concentration leads to higher energy density at low rates and lower energy density at high rates. Based on this we chose 0.5M LiAlCl$_4$ for the low rate cells, 1.0M LiAlCl$_4$ for the medium rate and 1.8M for the high rate cells. In this paper we discuss only the low and the medium rate cells.

In terms of electrode geometry, we investigated both the 'bobbin' and the wound types and found that the cathode reaction profiles and the electrolyte distribution of the bobbin type of electrodes were considerably inferior to those of the wound type of electrode structures, and as such the D cells with the bobbin type of electrode delivered significantly lower energy density than the D cells with wound electrodes. Furthermore, the D cells with the former type of electrodes were reported [4] to be sensitive to the cell orientation, whereas the latter type is not. For these reasons we chose the wound electrode geometry for further optimization. Our approach was an experimental one [10] rather than a computational one [4], and we carried out a detailed factorial experiment using hermetic D cells having various electrode areas and electrolyte salt concentrations, in an effort to develop a D cell with a maximal energy density at low rates. The discharge characteristics of the optimized cells are shown in Fig. 6. These cells were made with 4.45 cm (1.75 in.) wide and 25.4 - 38.1 cm (10 - 15 in.) long electrodes and 0.5M LiAlCl$_4$–SOCl$_2$ electrolytes. These cells delivered 18 - 19 A h at 0.01 A at 3.5 V, corresponding to energy densities of 20 W h/in.^{3} (1.24 W h/cm^3) and 300 W h/lb. (661 W h/kg). The SOCl$_2$ utilization as a function of the current density of these cells, as shown in Fig. 7, indicates utilization efficiencies approaching 100% at the lower current densities. This, therefore, represents the upper limit of the realizable energy density of the D size Li/
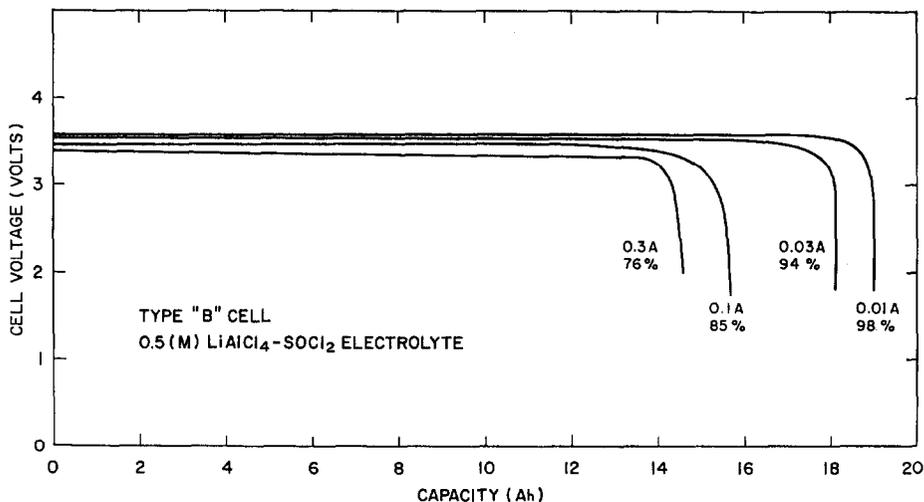
Fig. 6. Discharge curves of optimized low rate Li/SOCl$_2$ D cells at 25 °C, at currents of 0.3, 0.1, 0.03 and 0.01 A.
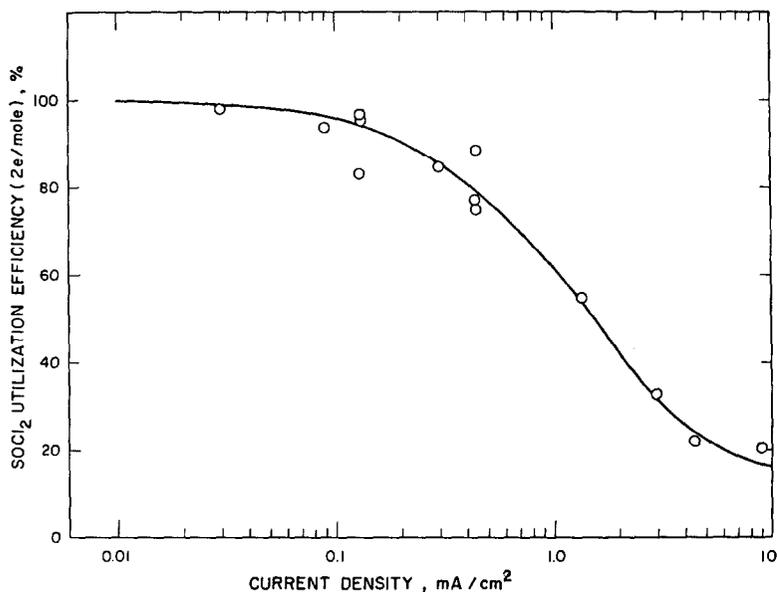
Fig. 7. SOCl$_2$ utilization efficiency of the optimized low rate cells as a function of current density.

SOCl$_2$ cell. The medium rate cells [11] were made with 50.8 cm (20 in.) long electrodes and 1.0M LiAlCl$_4$–SOCl$_2$ electrolyte, and these delivered maximum energy densities of 13 W h/in.^{3} and 190 W h/lb. (0.81 W h/cm^3 and 418 W h/kg) although this energy density remains virtually constant up to 1.0 A. The SOCl$_2$ utilization efficiency corresponding to the above maximum energy density is 70 - 75%. This indicates that significant improvement in the performance of the medium rate cells may be possible by further optimization of the cell with respect to its rate capability. The performance characteristics of both the low rate and the medium rate cells are shown in Fig. 8.

Storability

The high temperature storability of the system was found to be controlled by the spontaneous reaction of the Li anode with the electrolyte consisting of LiAlCl$_4$–SOCl$_2$, which resulted in the formation of an LiCl film on the anode. The latter caused instantaneous polarization of the cell on load followed by a slow recovery, particularly at low temperatures. The s.e.m. photographs of the bare Li and the passivated Li anode after passage of anodic current to recover voltage are shown in Figs. 9 and 10, respectively. The voltage recovery was due to the mechanical breakdown of the film after the Li had been anodically dissolved through pores. These openings were found only in a few places on the anode. Thus, both the film thickness and the morphology were important in determining the voltage-delay characteris-
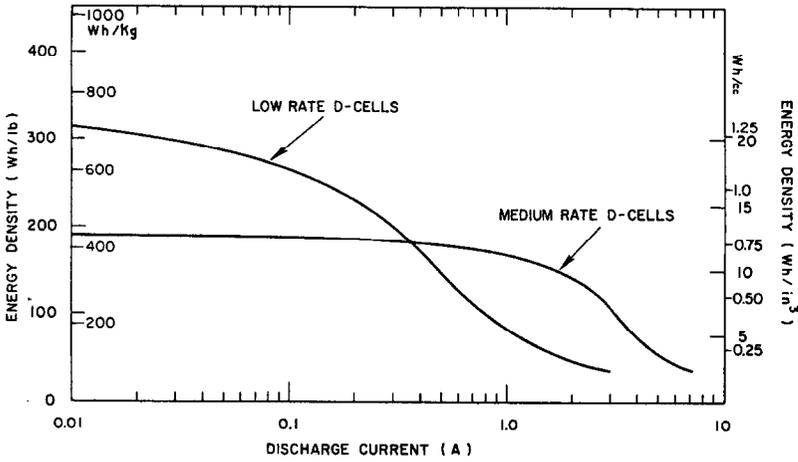
Fig. 8. Performance characteristics of low rate and medium rate Li/SOCl$_2$ D cells at 25 °C.
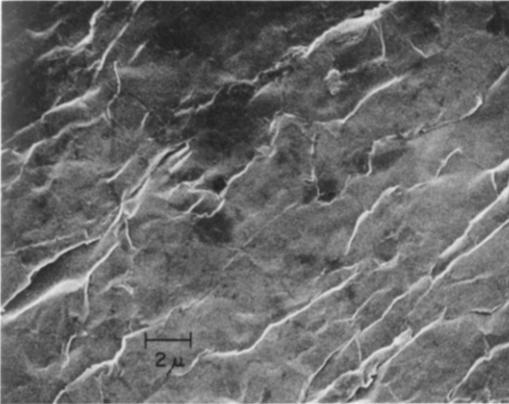
Fig. 9. S.e.m. photograph of bare Li surface (Magnification, × 1000).
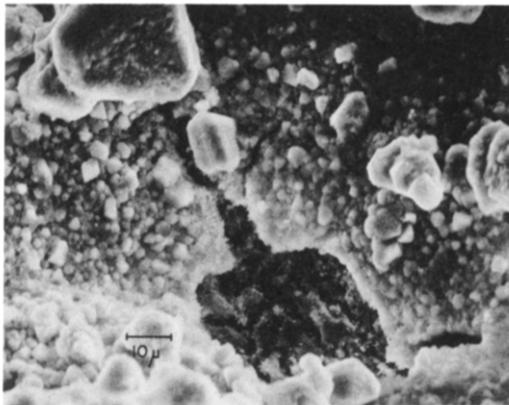
Fig. 10. S.e.m. photograph of Li surface after anodic polarization and voltage recovery showing the film cracking (Magnification × 1000).

tics of the Li anode. We carried out a systematic study of the kinetics and the morphology of the anode film growth as a function of various electrolyte variables. We found [8] that the $LiAlCl_4$ concentration in $SOCl_2$ affected the kinetics of the film growth, whereas additives such as SO_2 affected the morphology of the film growth. Use of electrolytes containing a judicious mixture of the above electrolyte variables led to a considerable improvement in the storability of the hermetic D cells. Improvements in the voltage delay have also been achieved [12, 13] by altering the electrolyte salt.

Cells with $Li_2B_{10}Cl_{10}$–$SOCl_2$ electrolyte were found [19] to exhibit substantially improved voltage-delay characteristics after storage. The conductivities of the conventional $LiAlCl_4$–$SOCl_2$ electrolyte and the $Li_2B_{10}Cl_{10}$ –$SOCl_2$ electrolyte at various temperatures and salt concentrations are shown in Fig. 11. Note that the conductivity of the latter electrolyte is somewhat lower than the conventional electrolyte. The cells with the latter electrolyte also showed significant capacity reduction after storage at 72 °C.

The general consensus [8, 14, 15] in regard to the mechanism of Li anode film growth is that the Li anode becomes covered with a very thin film of ionically conductive LiCl as soon as it contacts $SOCl_2$. We call this the *primary film*. Initially, this film is sufficiently thin to permit current flow without a substantial voltage drop, thus explaining the absence of voltage-delay of fresh cells. On storage there is a growth of a *secondary* crystalline film on top of the primary film. The growth is dependent upon both the electrolyte variables (such as electrolyte salt, electrolyte additives, electrolyte impurities) and the nature of the primary film on the Li anode (such as surface films of Li_2O, Li_3N and Li_2CO_3 which are present prior to its coming
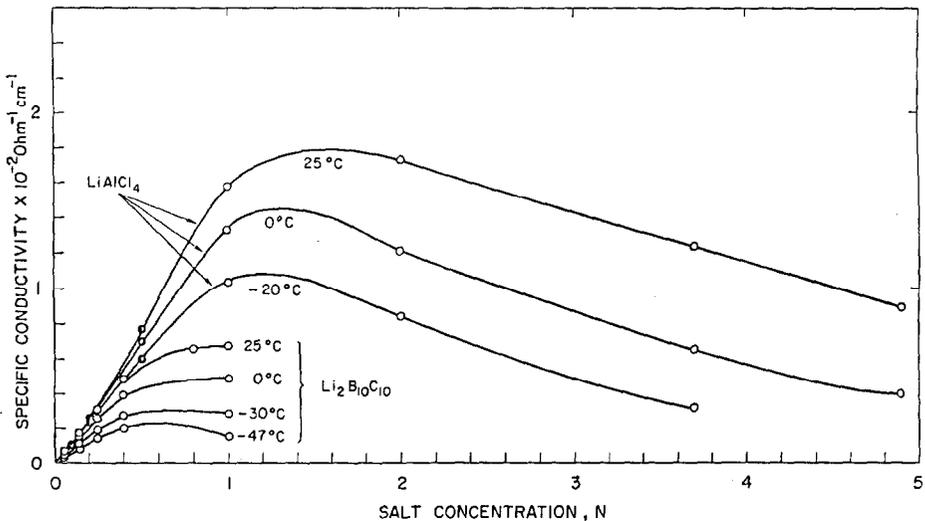
Fig. 11. Specific conductivity of $LiAlCl_4$–$SOCl_2$ and $Li_2B_{10}Cl_{10}$–$SOCl_2$ electrolytes as a function of salt concentration and temperature.

into contact with $SOCl_2$). Since LiCl occupies a larger volume than the original Li metal, it is likely that mechanical stresses in the LiCl film may lead to cracking of the primary film. The subsequent growth of the film in the form of large clusters of crystals [16] may occur due to local cell action through these cracks by a mechanism [8] involving both ionic transport through the cracks and electronic conduction in the primary LiCl film. The latter may be attributed to impurities incorporated in the film from the electrolyte.

The glass-to-metal seals used for the terminal of the hermetic cells were found to degrade and leak when partially discharged cells were stored. The degradation was found to be enhanced by the temperature and the duration of storage. The seals of the cells with $LiAlCl_4-SOCl_2$ electrolyte did not degrade or leak on storage as long as the cells were undischarged; only the partially and completely discharged cells exhibited this phenomenon. However, the seals of the cells with $Li_2B_{10}Cl_{10}-SOCl_2$ electrolyte degraded and leaked on storage even when they were undischarged. Examination of the seals revealed that the degradation occurred at the negative terminal of the cell. We believe that at the negative terminal the reduction of the metal and silicon oxides occurs according to

$$M_xO_y + 2YLi^+ + 2Ye \longrightarrow XM + YLi_2O \tag{5}$$

$$SiO_2 + 4Li^+ + 4e \longrightarrow 2Li_2O + Si \tag{6}$$

which results in the increase in the volume of the solids from 26 cm^3 for SiO_2 to 42 cm^3 for Li_2O and Si. This causes the glass to crack and leads to further penetration of the electrolyte through the cracks and reactions (5) and (6) causing further cracks along the negative terminal. The nature of the electrolyte appears to affect the reduction process. This seal degradation problem can be solved by a proper choice of seal materials, and state-of-the-art cells are now capable of withstanding storage durations approaching one year at 72 °C in a partially and/or completely discharged state without any leakage through the glass-to-metal seal. The partially discharged cells with conventional glass-to-metal seals leaked within a month of storage at 72 °C.

Safety

Li/$SOCl_2$ batteries were found to explode under the following conditions.
    (a) short circuiting,
    (b) force-discharge (reversal)
    (c) casual storage and/or exposure to the environment of a partially discharged cell.
Accidental short circuiting of a high rate cell [7] leads to excessive cell heating which caused the explosion. The problem is preventable by the use of low pressure venting (0.7 - 1.4 MPa (100 - 200 psi)) which causes the cells to cool down sufficiently before they reach the critical temperature, thus preventing cell explosion. A schematic diagram of a typical hermetic low pres-

sure vent [20] for the D cells is shown in Fig. 12. The vent comprises a metal disc covering a hole on the metal cell top and is bonded to the metal cell top by means of a glass, very similar to that of a glass-to-metal seal. The pressure at which the glass-to-metal bond is broken resulting in cell venting is determined both by the diameter of the hole and the stiffness of the cell top. On slight bending of the cell top when the internal pressure reaches approximately 0.7 MPa (100 psi), the metal disc separates from the glass thus opening the hole on the cell top through which the cell vents. The configuration of the vent disc is such that it cannot be opened by external pressure. Another advantage of this type of vent is that the size of the opening of the vent can be kept fixed by design. Typical wall temperature–time plots of medium rate D cells on shorting at 25 and 72 °C are shown in Fig. 13. The temperature rose first and declined rapidly after the vent opened and there was no explosion. However, venting may not be a desirable consequence under many circumstances, although it may be more desirable than an explosion. The low rate cells discussed above do not undergo an explosion on shorting, and as such, a safety vent may not be needed for them.
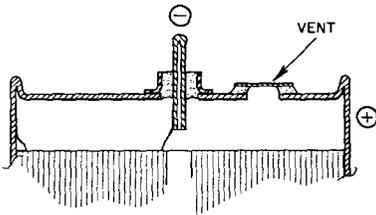
Fig. 12. Schematic diagram of the low pressure hermetic vent.
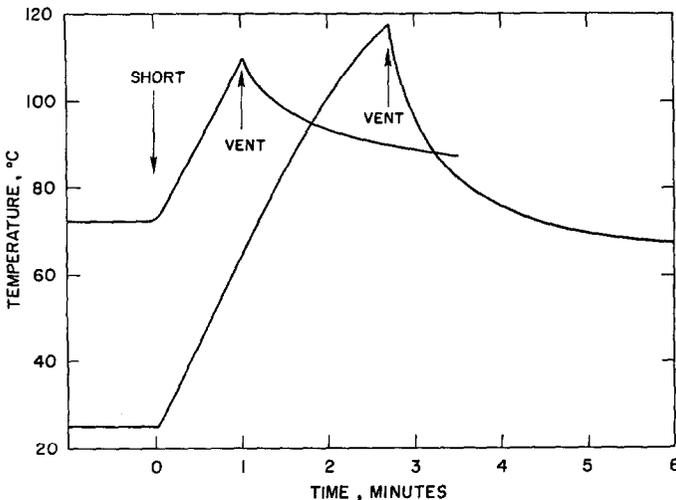
Fig. 13. Wall temperature–time plots of medium rate Li/SOCl$_2$ D cells with low pressure vent on shorting at 25 and 72 °C.

On force-discharge (which a defective cell may encounter in a multicell battery) the medium rate cells exploded in spite of a vent. We solved this problem by modifying the electrode designs. The voltage and the temperature plots of a modified medium rate D cell on 1 A discharge and force-discharge for 90 h are shown in Fig. 14. The cells were found to be extremely abuse resistant. However, at the end of such prolonged force-discharge (reversal), the cells tend to become percussion sensitive. We do not expect such prolonged reversal under any normal use conditions and the percussion sensitivity may not be a real problem.

A detailed study was undertaken to solve the problems of explosion of partially discharged cells during casual storage and/or exposure to the environment. Microcalorimetry [17] of Li/SOCl$_2$ D cells showed that the cells continue to produce heat after discharge. This indicates that 'instability' is generated as a result of the discharge. We characterized this instability by doing d.t.a. (differential thermal analysis) of discharged D cells against a reference. The d.t.a. fixture is shown in Fig. 15. The thermogram of an undischarged cell against a reference showed no transitions, whereas the thermogram of a discharged cell against the reference showed two exothermic transitions (Fig. 16). These exothermic transitions disappeared on the subsequent d.t.a. run indicating that the exotherms are due to the reaction of unstable chemicals formed during the discharge. Based on this, it is suggested that the 'instability' of partially discharged cells may be removed by a controlled thermal treatment which may prevent explosion on casual storage.

Detailed d.t.a. of all the possible chemicals present in the cells and the 'exothermicity' measurements [18] indicate that chemical species such as Li$_2$S (which may be formed by reaction of S + Li) can react explosively with
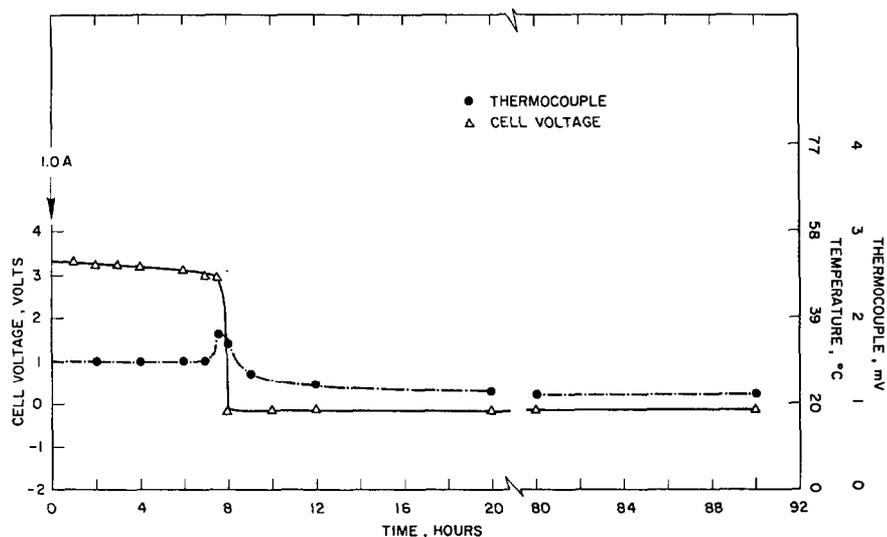
Fig. 14. Voltage and wall temperature profiles of a modified medium rate Li/SOCl$_2$ D cell on 1.0 A discharge and force-discharge.
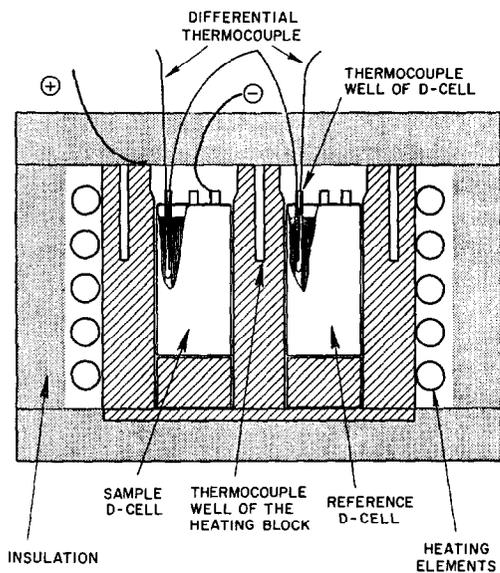
Fig. 15. Fixture for doing d.t.a. (differential thermal analysis) of Li/SOCl$_2$ D cells.
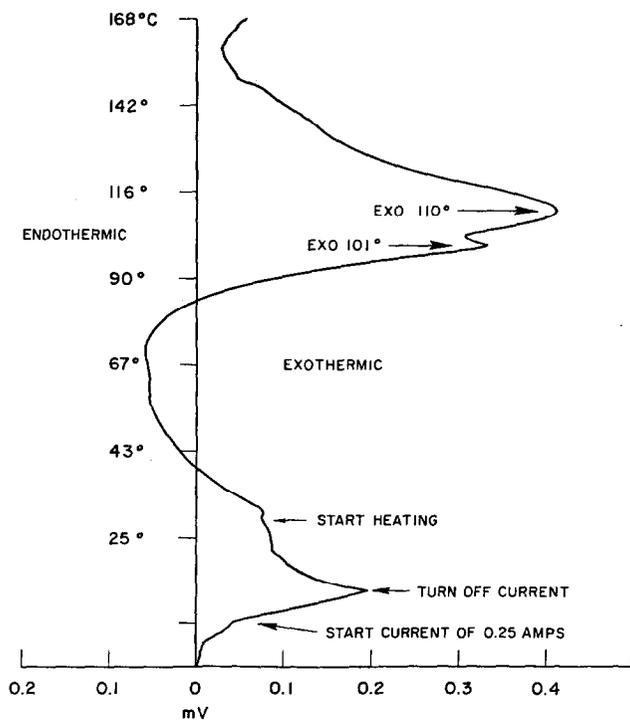
Fig. 16. D.t.a. thermogram of a discharged Li/SOCl$_2$ D cell (12.3 A h) against Al$_2$O$_3$ reference.

$SOCl_2$, producing heat. Thus, exposure to the environment may cause ingress of moisture and spontaneous cell heating leading to an explosion. Therefore, total hermeticity of cells under all conditions of test and storage must be maintained for safety of these cells.

Conclusions

Hermetically-constructed $Li/SOCl_2$ D cells were used for the studies reported in this publication. Optimization of the cells with respect to energy density was carried out by studying the effect of cell construction parameters, such as type of carbon in the cathode, electrode areas (and thicknesses), and electrolyte salt concentration, on the energy density of the spirally-wound D cells. The optimized D cells delivered 18 - 19 A h at 3.5 V at 25 °C, at 0.01 A corresponding to energy densities of 20 W h/in.^{3} (1.24 W h/cm^3) and 300 W h/lb. (661 W h/kg). The optimization of the cells with respect to storability was carried out by studying the effect of electrolyte salt concentration, electrolyte salt types, and electrolyte additives on the Li anode film growth rate and morphology as a function of storage temperature and storage duration. The D cells with optimized electrolyte showed no voltage-delays after three months of storage at 72 °C and test at −30 °C at 3.0 A. The optimization of the cells with respect to safety was carried out by developing low pressure vents and by studying the thermal characteristics of the cell constituents as well as the D cells, using differential thermal analysis. The optimized cells were found to be resistant to abuses such as shorting and force-discharge. In addition, approaches have been developed to stabilize the partially-discharged cells and thus prevent spontaneous explosions on storage.

Acknowledgements

References

1 W. K. Behl, J. A. Christopulos, M. Ramirez and S. Gilman, *J. Electrochem. Soc.*, *120* (1973) 1619.
2 J. J. Auborn, K. W. French, S. I. Lieberman, V. K. Shah and A. Heller, *J. Electrochem. Soc.*, *120* (1973) 1613.
3 A. N. Dey and C. R. Schlaikjer, *Proc. 26th Power Sources Symp., Atlantic City, N.J., 1974.*
4 N. Marincic, *J. Appl. Electrochem.*, *6* (1976) 51, 263.

5 J. R. Driscoll, G. L. Holleck and D. E. Toland, *Proc. 27th Power Sources Symp., Atlantic City, N.J., 1976,* The Electrochemical Society, Princeton, N.J.

6 C. Schlaikjer, F. Goebel and N. Marincic, *Electrochemical Society Fall Meeting, Atlanta, Georgia,* The Electrochemical Society, Princeton, N.J., Abstract No. 16.

7 A. N. Dey, *J. Electrochem. Soc., 123* (1976) 1 262.

8 A. N. Dey, *Thin Solid Films, 43* (1977) 131.

9 A. N. Dey and P. Bro, *J. Electrochem. Soc., 125* (1978) 1 574.

10 A. N. Dey and P. Bro, in D. H. Collins (ed.), *Power Sources 6,* Academic Press, London, 1977, p. 493.

11 A. N. Dey, *Electrochim. Acta, 21* (1976) 855.

12 C. R. Schlaikjer, *Proc. 28th Power Sources Symp., Atlantic City, N.J., 1978,* The Electrochemical Society, Princeton, N.J.

13 J. P. Gabano, P. Lenfant, *Electrochemical Society Fall Meeting, Pittsburgh, Pa., Oct. 15 - 20, 1978,* The Electrochemical Society, Princeton, N.J., Abstract No. 27.

14 E. Peled, *Proc. 28th Power Sources Symp., Atlantic City, N.J., 1978,* The Electrochemical Society, Princeton, N.J.

15 R. V. Moshtev, Y. Geronov, G. Puresheva and A. Nasalevska, *28th ISE Meeting,* Druzhba, Varna, Bulgaria, Sept., 1977, Extended Abstract No. 153.

16 A. N. Dey, *Electrochim. Acta, 21* (1976) 377.

17 P. Bro, in J. Thompson (ed.), *Power Sources 7,* Academic Press, 1979, p. 571.

18 A. N. Dey, *Proc. 28th Power Sources Symp., Atlantic City, N.J., 1978,* The Electrochemical Society, Princeton, N.J.

19 A. N. Dey and J. Miller, *J. Electrochem. Soc., 126* (1979) 1 445.

20 A. N. Dey and J. H. Him, *U.S. Patent 4 115 629,* Sept. 19, 1978.